



Molecular Crystals and Liquid Crystals

Publication details, including instructions for authors and subscription information:

<http://www.tandfonline.com/loi/gmcl20>

All-Optical and Thermal Tuning of a Bragg Grating Based on Photosensitive Composite Structures Containing Liquid Crystals

G. Gilardi^a, R. Asquini^a, A. d'Alessandro^a, R. Beccherelli^b, L. De Sio^c & C. Umeton^c

^a Department of Information Engineering, Electronics and Telecommunications, Sapienza University of Rome Via Eudossiana, 18 00184, Rome, Italy

^b Consiglio Nazionale delle Ricerche - Istituto per la Microelettronica e Microsistemi Via del Fosso del Cavaliere, 100 - 00133, Rome, Italy

^c LICRYL (Liquid Crystals Laboratory, CNR - IPCF), Center of Excellence CEMIF.CAL and Department of Physics University of Calabria, 87036, Arcavacata di Rende (CS), Italy

Version of record first published: 18 Apr 2012.

To cite this article: G. Gilardi, R. Asquini, A. d'Alessandro, R. Beccherelli, L. De Sio & C. Umeton (2012): All-Optical and Thermal Tuning of a Bragg Grating Based on Photosensitive Composite Structures Containing Liquid Crystals, *Molecular Crystals and Liquid Crystals*, 558:1, 64-71

To link to this article: <http://dx.doi.org/10.1080/15421406.2011.653680>

PLEASE SCROLL DOWN FOR ARTICLE

Full terms and conditions of use: <http://www.tandfonline.com/page/terms-and-conditions>

This article may be used for research, teaching, and private study purposes. Any substantial or systematic reproduction, redistribution, reselling, loan, sub-licensing, systematic supply, or distribution in any form to anyone is expressly forbidden.

The publisher does not give any warranty express or implied or make any representation that the contents will be complete or accurate or up to date. The accuracy of any instructions, formulae, and drug doses should be independently verified with primary sources. The publisher shall not be liable for any loss, actions, claims, proceedings, demand, or costs or damages whatsoever or howsoever caused arising directly or indirectly in connection with or arising out of the use of this material.

All-Optical and Thermal Tuning of a Bragg Grating Based on Photosensitive Composite Structures Containing Liquid Crystals

G. GILARDI,^{1,*} R. ASQUINI,¹ A. d'ALESSANDRO,¹
R. BECCHERELLI,² L. DE SIO,³ AND C. UMETON³

¹Department of Information Engineering, Electronics and Telecommunications,
Sapienza University of Rome Via Eudossiana, 18 00184 Rome – Italy

²Consiglio Nazionale delle Ricerche – Istituto per la Microelettronica e
Microsistemi Via del Fosso del Cavaliere 100 – 00133, Rome – Italy

³LICRYL (Liquid Crystals Laboratory, CNR – IPCF), Center of Excellence
CEMIF.CAL and Department of Physics University of Calabria 87036,
Arcavacata di Rende (CS), Italy

We report on the fabrication and characterization of a tunable filtering effect, observed in a waveguide grating made of alternated strips of photocurable polymer and a mixture of azo-dye doped liquid crystal. The grating is sandwiched between two borosilicate glasses, one of which includes an ion-exchanged channel waveguide, which confines the optical signal to be filtered. We analyze the effects of a low power visible, pump light beam that hits the sample and temperature effects. Both effects are investigated experimentally. The application of the pump light allowing the filtered wavelength to be tuned over a 6.6 nm range, while a temperature variation of 4° C, implies a tuning of 14 nm.

Keywords Optical waveguides; liquid crystals; opto-optical effect

Introduction

Bragg reflectors are periodic structures that play important functions in integrated optics. They can be used in various applications including tunable lasers [1], polarization dispersion compensation and manipulation [2], spectrometry [3], multi/demultiplexing [4], sensing [5], and spectral filtering [6]. Bragg reflectors have been demonstrated by employing waveguides made of different materials and structures such as polymers [7], silicon-on-insulator (SOI) [8], hollow capillaries [2], lithium niobate [9], metal-insulator-metal [10] silica [11] and liquid crystals [12,13]. Such reflectors can be tuned by using different mechanisms such as thermo-optic [14], mechanical [15], electrical [11] acousto-optical [9], electro-optical [12,13] or opto-optical [16].

Recently, composite organic materials, such as azo-dye doped liquid crystals, have been engineered to obtain all-optical effects which proved very efficient in terms of switching speed and low driving optical power [17,18].

*Address correspondence to G. Gilardi, Department of Information Engineering, Electronics and Telecommunications, Sapienza University of Rome Via Eudossiana, 18 00184 Rome – Italy

Furthermore, micro/nano structured templates designed to realize a generation of holographic gratings called POLICRYPS (POLimer LIquid CRYstal Polymer Slices) based on polymers and liquid crystals (LC) [19,20] have been combined with such azo compounds to obtain efficient, optically controllable, free-space devices [21]. POLICRYPS represent a low cost and easy to fabricate approach to make efficient Bragg reflectors with respect to other technologies. In order to envisage a generation of low cost and low driving power, easy to fabricate, all optical devices, in this paper we propose and experimentally demonstrate an integrated all-optical tuneable filter. It is obtained by combining a simple and low cost ion-exchange waveguide technology with a composite LC and a well characterized photosensitive azo-dye compound, methyl red (MR), to enable full optical tuning in the telecom wavelength range.

Device Fabrication

A schematic illustration of the proposed device is in Fig. 1. The first fabrication step consists of a double ion-exchange process ($\text{KNO}_3\text{-AgNO}_3$) to obtain a channel optical waveguide on a BK7 substrate as described in [22]. The device is then assembled by placing a BK7 glass cover on the top of the processed substrate (which includes the optical channel waveguide) by using ball spacers of about $1\ \mu\text{m}$ in diameter, mixed to an UV-curable glue to control the gap. In the first step, the POLICRYPS structure is realized according to the standard fabrication process [19]. Then, it is possible to realize a polymeric template by etching the POLICRYPS structure using the multi-step process, in which the NLC is removed by using a microfluidic etching process, and the obtained polymeric template can be filled with self-organizing materials. This technique provides two striking advantages: it is completely insensitive to dust particles because the polymerization occurs in an already sealed device and the polymer symmetrically adheres to both glass substrates leaving no gaps. We, infiltrated the polymeric structure with nematic LC (NLC) E7 doped with MR, 2% in weight. Such a percentage has been chosen by considering the highest possible

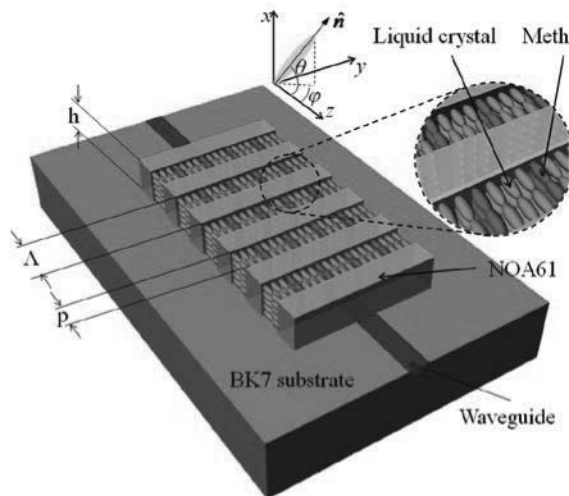


Figure 1. Schematic view of the proposed device with a zoom on the grating structure. The top inset sketches the orientation tilt (θ) and twist (ϕ) angles of the molecular director \hat{n} .

solubility of MR in NLC (MR:E7) to minimize the pump power required for the optical switching [21].

Working Principle

According to the Bragg law, the back-reflected wavelength is given by:

$$\lambda_B = 2\Lambda n_{eff}/m \quad (1)$$

Where λ_B is the back-reflected wavelength, $\Lambda = 1.5 \mu\text{m}$ is the period of the grating, $m = 3$ is the diffraction order and n_{eff} is the effective refractive index of the propagating mode. Λ and m are imposed by the fabrication, then to obtain the tuning of the device we can act on n_{eff} . It depends on the ion diffusion profile in the glass, on the upper glass refractive index, on the overlayer refractive index and on its thickness. The overlayer thickness is imposed by the fabrication ($h \approx 1 \mu\text{m}$). To tune the device we can only modify the effective refractive index of the grating.

The refractive indices of E7 NLC are well characterized, with values at $\lambda = 1550 \text{ nm}$ which are $n_{||} = 1.689$ and $n_{\perp} = 1.5$ for light polarization parallel and perpendicular to the LC director, respectively. The period of the grating fabricated for the realization of the optical filter is estimated to be $\Lambda = 1.50\text{--}1.55 \mu\text{m}$. For $m = 3$ the value of λ_B is in the telecom wavelength range of $1520\text{--}1570 \text{ nm}$.

All-Optical Tuning: Experiments and Simulations

At the thermal equilibrium, without any applied external stimulus, the MR is in its elongated *trans* form. The MR:E7 behaves as guest-host optically anisotropic mixture of a liquid crystalline compound and a non-liquid crystalline compound. In this mixture, the long axis of the LC molecules and long axis of *trans*-MR remain parallel to z -axes, as in all POLICRYPS structures [20]. This is easily verified by an investigation through the polarized microscope.

Due to the mismatch between the *trans* MR: E7 ordinary refractive (≈ 1.5 at 1550 nm [23]) index and the index of the NOA61 polymer (1.5419 at 1550 nm [24]) in the overlaying grating, a TE-like optical beam guided by the waveguide experiences a phase grating. This enables the device to operate as a Bragg filter.

Since the absorption band of *trans* isomer is typically in the green range, the MR turns in the spherical *cis* form when the grating is irradiated by a green light beam $\lambda = 532 \text{ nm}$. Such conformational transition brakes the directional order of the MR-E7 guest-host. In this condition, the NLC:MR mixture behaves like a typical optically isotropic material, as easily verified by an optical analysis using a polarized microscope. The refractive index of the mixture after exposure can be estimated as the average value given by [25]:

$$\langle n \rangle = \sqrt{\frac{n_{||}^2 + 2n_{\perp}^2}{3}} = 1.5655 \quad (2)$$

There is therefore, a mismatch with the polymer refractive index and a variation in the value of the back-reflected Bragg wavelength. Figure 2 shows the all-optical setup used to measure the transmitted spectra of this tuneable filter.

The input and output end facets of the device are butt-coupled to a single mode fiber. The input signal is supplied by an erbium doped fiber amplifier operating in the wavelength

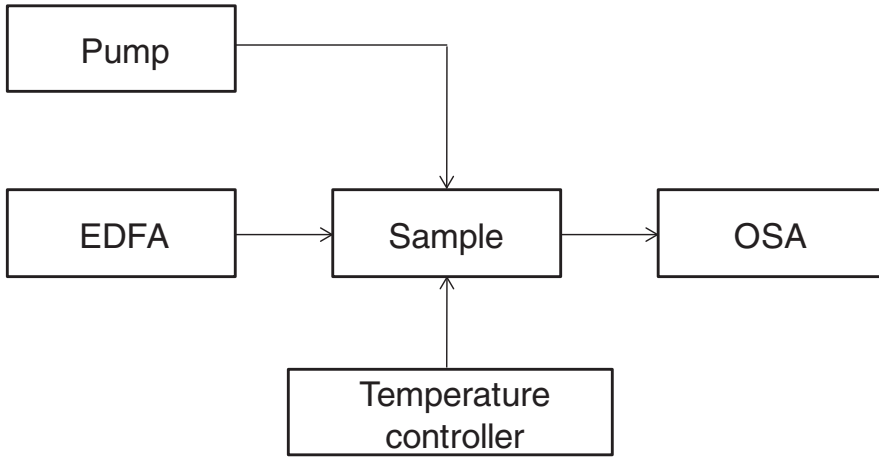


Figure 2. Setup used to measure the transmitted spectra.

range between 1520 and 1580 nm. A single mode fiber butt-coupled to the output end-face of the waveguide is used to send the filtered output light signal to an optical spectrum analyser. The pump laser has a circular spot (about 2 mm in diameter) and a power of 45 mW at $\lambda = 532$ nm, a value that greatly exceeds the threshold of the *trans-cis* transition.

Figure 3 shows the transmitted spectrum, which exhibits a notch peak of -20 dB at the wavelength $\lambda = 1545.7$ nm when the pump is off (black line). When the pump is on, the spectrum is shifted by $\Delta\lambda_B = 6.6$ nm (red line), preserving its shape but with a slightly deeper notch of about -22 dB. The bandwidth of the transmitted notch, considered at -3 dB with respect to the transmittance minimum value, is 3.3 nm when the pump is OFF and 2.7 nm when the pump is ON. We have used eq. (1) to perform computer simulations of the behavior of the filter in three basic steps. In the first step, we studied the orientation

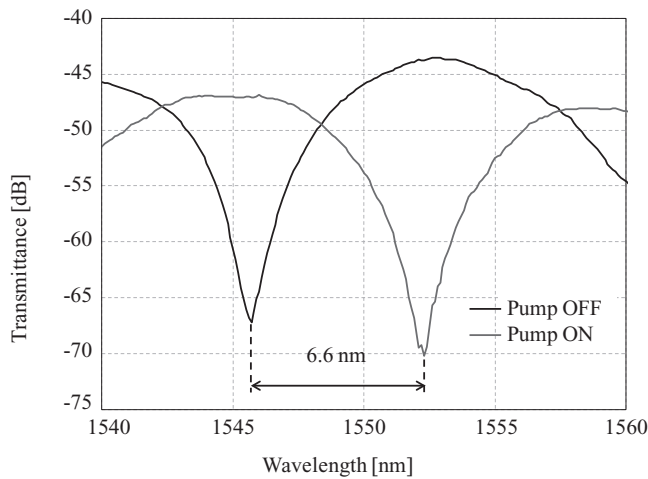


Figure 3. Transmitted spectra of the POLICRYPS all-optical filter. Black line – Pump off; inset with azo dye in *trans*-phase. Red line – Pump on; inset with azo dye in *cis*-form. Both measurements have been taken at 20.8°C.

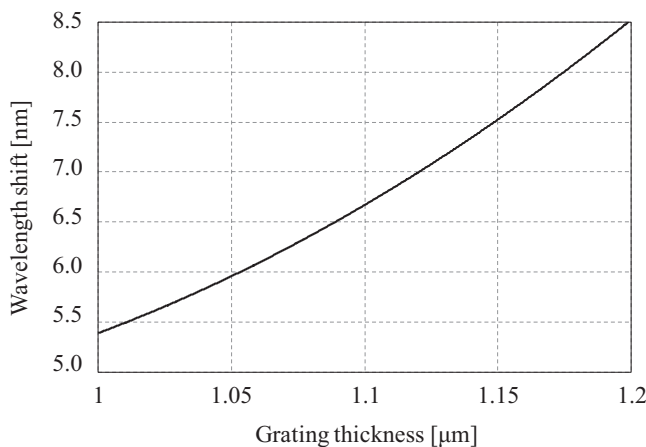


Figure 4. Relation between wavelength shift and grating thickness for the pump laser power of 45 mW at $\lambda = 532$ nm.

angle of the NLC director comprised between the NOA61 stripes in the POLICRYPS structure. The director profile was computed minimizing the LC free energy by solving the partial derivate Euler-Lagrange equation of the free energy implemented in the weak form by means of a finite element method. The terms to take into account in the minimization of the free energy are: i) the elastic energy of the LC that depends on its elastic constants, ii) mechanical orientation induced by the MR deformation, as result of the applied external pump.

In the second step, the NLC refractive index distribution derived from the director profile was used to describe the grating by a grating mode solver [26]. The effective index computed in the second step is used in the third step to solve equation (1).

In the simulation, we consider several different values of the grating thickness to include a low uncertainty in the estimation of the device gap. The result is reported in Fig. 4 and the wavelength shift obtained numerically is $\Delta\lambda_{B1} = 5.88$ nm for $h = 1$ μm , $\Delta\lambda_{B2} = 7.25$ nm for $h = 1.1$ μm and $\Delta\lambda_{B3} = 9.19$ μm for $h = 1.2$ μm .

It is evident that an increase of h yields an increase of $\Delta\lambda_B$, for the same value of the refractive index. This behavior can be explained in terms of a smaller influence of the boundary conditions.

Initially, the NLC director is considered to be parallel to the z direction (Fig. 1), so that a TE-like input light experiences the n_{\perp} index of the NLC. The exposure to the green light makes the reorientation of the NLC molecules not uniform, due to the presence of MR, hence the NLC can be considered isotropic and the average value of E7 refractive index $\langle n \rangle = 1.5655$ according to eq. 2 is used in the calculations. The model takes into account also the interaction of the NLC with glass and NOA61. In particular, a pretilt angle of 2° is imposed in the calculations, in order to avoid the presence of a Fréedericks threshold for the director orientation. Finally, a pretwist angle of $\approx 0^\circ$ is set at the normal orientation of n in the liquid crystal-NOA61 interface.

Figure 4 highlights that a wavelength shift value about 6.6 nm, is obtained for a thickness of approximately 1.1 μm , in agreement with the experimentally measured shift and the gap of the realised sample.

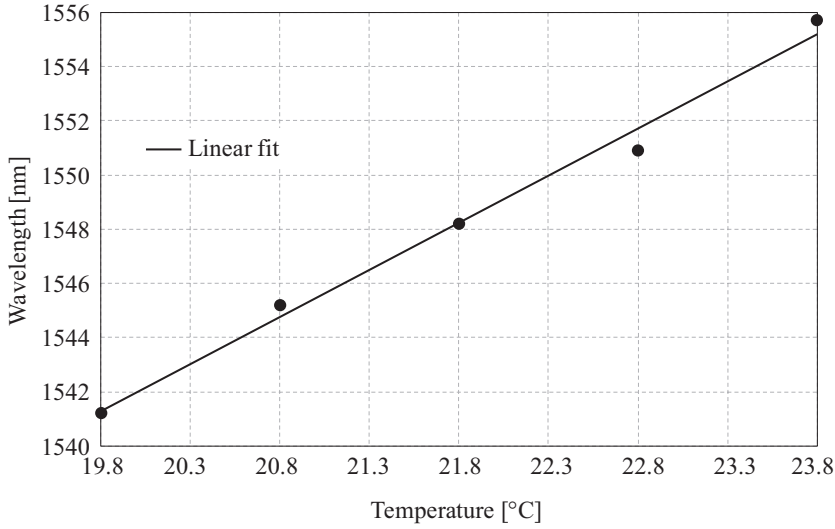


Figure 5. Wavelength shift as a function of the temperature with the laser pump OFF.

Thermo-Optical Tuning: Experiments

As shown in Fig. 3, the sample under investigation is positioned over a heater. The temperature of the sample is controlled by the application of a proper current in the heater. The experimental result of the thermal effect is represented in Fig. 5.

Figure 5 shows that the wavelength shift with the temperature is well described by a linear curve. The resonant wavelength shifts from 1541 nm to 1555 nm, when the sample temperature changes from 19.8°C to 23.8°C.

The temperature variation of all materials involved in the structures implies a change in their refractive index. The bottom glass and the upper glass do not have an important role in the definition of the wavelength shift with the temperature because their low thermo-optical coefficient (about $-10^{-6}/^{\circ}\text{C}$) [27]. The MR does not influence n_{eff} , due to its relative low percentage in the NLC:MR mixture. The increase of temperature modifies the refractive index difference between the NOA61 and the MR:E7 mixture because they have different thermo-optical coefficients. The thermo-optical coefficient for the NOA61 is about $-10^{-3}/^{\circ}\text{C}$ [24]. In the NLC both n_{\perp} and n_{\parallel} depend on the temperature. In particular n_{\parallel} decreases, while n_{\perp} increases when the temperature increases. In this mixture, the long axis of the LC remains parallel to z -axes therefore, only n_{\perp} must be considered. The thermo-optical coefficient for n_{\perp} is greater than the NOA61 thermo-optics coefficient and it is also positive [28]. The total effect induced by the temperature increase is the increase of n_{eff} then a red-shift of the resonant wavelength.

Conclusion

In conclusion, we have demonstrated an all-optical Bragg filter integrated on glass by using commercially available materials, combining ion exchanged channel waveguides and composite holographic gratings. The prototype exhibits a signal suppression higher than 20 dB at the Bragg wavelength, with a bandwidth of the transmitted notch of about 3 nm. A

tuning range of 6.6 nm is observed by applying a pump green light of 45 mW. The device exhibit a red-shift of 14 nm due to a temperature variation of 4°C.

A simple model, implemented to carry out numerical simulations, yields values of the Bragg wavelength shift which are in full agreement with our measurements. An improve of the proposed device is related to changes in the grating pitch to obtain operation at the first order of diffraction and in the use of new, high performance, mesogenic LC to obtain a reduction of the pump laser energy.

Acknowledgments

This research has been partially supported by the Air Force Office of Scientific Research, Air Force Material Command, U.S. Air Force, under grant FA8655-07-1-3046 and by PRIN 2006 - Umeton - prot. 2006022132_001.

References

- [1] Noh, Y. O., Lee, H. J., Ju, J. J., Kim, M. S., Oh, S. H., & Oh, M. C. (2008). *Opt. Express*, 16, 18194–18201.
- [2] Kumar, M., Sakaguchi, T., & Koyama, F. (2009). *Appl. Phys. Lett.*, 94, 061112.
- [3] DeCorby, R. G., Ponnampalam, N., Epp, E., Allen, T., & McMullin, J. N. (2009). *Opt. Express*, 17, 16632–16645.
- [4] Brouckaert, J., Bogaerts, W., Selvaraja, S., Dumon, P., Baets, R., & Van Thourhout, D. (2008). *Photon. Technol. Lett.*, 20, 309–311.
- [5] Jalkanen, T., Torres-Costa, V., Salonen, J., Björkqvist, M., Mäkilä, E., Martinez-Duart, J. M., & Lehto, V. P. (2009). *Opt. Express*, 17, 5446–5456.
- [6] Murphy, T. E., Hastings, J. T., & Smith, H. I. (2001). *J. Lightwave Technol.*, 19, 1938–1942.
- [7] Jeong, G., Lee, J. H., Park, M. Y., Kim, C. Y., Cho, S. H., Lee, W., & Kim, B. W. (2006). *IEEE Photon. Technol. Lett.*, 18, 2102–2104.
- [8] Brouckaert, J., Bogaerts, W., Selvaraja, S., Dumon, P., Baets, R., & Van Thourhout, D. (2008). *IEEE Photon. Technol. Lett.*, 20, 309–311.
- [9] Tian, F., Harizi, C., Herrmann, H., Reimann, V., Ricken, R., Rust, U., Sohler, W., Wehrmann, F., & Westenhofer, S. (1994). *J. Lightwave Technol.*, 12, 1192–1197.
- [10] Hosseini, A., & Massoud, Y. (2009). *Opt. Express*, 14, 11318–11323.
- [11] Lin, X. Z., Zhang, Y., An, H.-L., & Liu, H.-D. (1994). *Electron. Lett.*, 30, 887–888.
- [12] Gilardi, G., Asquini, R., d'Alessandro, A., & Assanto, G. (2010). *Opt. Express*, 18(11), 11524–11529.
- [13] Asquini, R., Gilardi, G., d'Alessandro, A., & Assanto, G. (2010). *Optical Engineering*, 50(7), 071108.
- [14] Jeong, G., Lee, J. H., Park, M. Y., Kim, C. Y., Cho, S. H., Lee, W., & Kim, B. W. (2006). *IEEE Photon. Technol. Lett.*, 18, 2102–2104.
- [15] Kim, K. J., Seo, J. K., & Oh, M. C. (2008). *Opt. Express*, 16, 1423–1430.
- [16] Ehrlich, J. E., Assanto, G., & Stegeman, G. I. (1990). *Appl. Phys. Lett.*, 56, 602–604.
- [17] Tabiryan, N., Hrozhyk, U., & Serak, S. (2004). *Phys. Rev. Lett.*, 93, 113901–113904.
- [18] Hrozhyk, U. A., Serak, S. V., Tabiryan, N., Hoke, L., Steeves, D. M., & Kimball, B. R. (2010). *Opt. Express*, 18, 8697–8704.
- [19] Caputo, R., De Sio, L., Veltri, A., Umeton, C., & Sukhov, A. V. (2004). *Opt. Lett.*, 29, 1261–1263.
- [20] Caputo, R., Veltri, A., Umeton, C. P., & Sukov, A. (2004). *J. Opt. Soc. Am. B*, 21(11), 1939–1947.
- [21] De Sio, L., Serak, S., Tabiryan, N., Ferjani, S., Veltri, A., & Umeton, C. (2010). *Adv. Mater.*, 22, 2316–2319.
- [22] Zou, J., Zhao, F., & Chen, R. T. (2002). *Appl. Opt.*, 41, 7620–7626.
- [23] Li, J., Wu, S. T., Brugioni, S., Meucci, R., & Faetti, S. (2005). *J. Appl. Phys.*, 97, 73501–73505.
- [24] <https://www.norlandprod.com/adhesives/NOA%2061.html>

- [25] Li, J., Gauza, S., & Wu, S. (2004). *J. Appl. Phys.*, 96, 1.
- [26] <http://www.rsoftdesign.com>.
- [27] Ghosh, G. (1997). *Appl. Opt.*, 36(7), 1540–1546.
- [28] Khoo, I. C. (2007). *Liquid Crystals (Second Edition)*, John Wiley & Sons.